Available online at www.sciencedirect.com
SCIENCE DIRECT®
Surface Science 573 (2004) 379–390
SURFACE SCIENCE
www.elsevier.com/locate/susc

Hydrophobic properties of surfaces coated with fluoroalkylsiloxane and alkylsiloxane monolayers

S.A. Kulinich [a,*], M. Farzaneh [a,b]

[a] *Canada Research Chair on Engineering of Power Network Atmospheric Icing, UQAC, Saguenay, QC, Canada G7H 2B1*
[b] *NSERC/Hydro-Quebec/UQAC Industrial Chair on Atmospheric Icing of Power Network Equipment, Saguenay, QC, Canada G7H 2B1*

Received 9 July 2004; accepted for publication 4 October 2004
Available online 21 October 2004

Abstract

A comparative analysis of hydrophobicity of fluoroalkylsiloxane and alkylsiloxane monolayers is presented. In order to compare wetting behavior on smooth and rough substrates, a simple model considering various self-assembly degrees of organic molecules and various area fractions of air inclusion is used. Sliding behavior for water on rough silanized needle-like surfaces is also evaluated. On smooth surfaces, regardless of assembly degree of coatings, contact angles of fluoroalkylsiloxane monolayers are always ~10° larger. The difference, however, decreases when rough substrates with air inclusion are used. It is shown that assembly order of silane molecules and reduced water–solid contact area are the key factors leading to both high contact angles and low sliding angles. Such coatings are expected to be potential snow- and ice-repellent materials.

Keywords: Surface energy; Surface structure, morphology, roughness, and topography; Wetting; Biological compounds; Self-assembly; Silane

1. Introduction

Wettability is an important property of solid surfaces from theoretical, practical, and technological points of view [1–10]. Fabrication of self-assembled monolayer (SAM) coatings is one of the most successful approaches to chemical modification and hydrophobization of many hydrophilic surfaces [1,5,9,11–16].

A class of widely used SAMs is based on *n*-alkyltrichlorosilane [5,15,17–19] or *n*-alkyltrialkoxysilane [10] precursor molecules, which, through a combined process of adsorption, hydrolysis, and polymerization can lead to spontaneously assembled, often highly organized, alkylsiloxane monolayer films with low surface energy at the surfaces of many solids, most notably oxides (Al_2O_3, SiO_2, SnO_2, TiO_2, silicate glasses, etc.).

* Corresponding author. Tel.: +1 418 545 5011x5053; fax: +1 418 545 5032.
E-mail address: skulinic@uqac.ca (S.A. Kulinich).

0039-6028/$ - see front matter © 2004 Elsevier B.V. All rights reserved.
doi:10.1016/j.susc.2004.10.008

Thus, various hydrophilic surfaces can be made hydrophobic by means of this process. As an example, octadecyltrichlorosilane, the most common model compound, self-assembles into a robust octadecylsiloxane (ODS) monolayer on almost any high-energy surface [15,17–19].

In order to form a complete monolayer, silane groups condense with surface hydroxyl groups to form a thin layer of polysiloxane. Therefore, to immobilize the organosilane monolayers on the substrate, the presence of OH groups on the surface is normally required. Fig. 1 (left) demonstrates self-assembly for a perfluorinated octylsiloxane (FAS-13) monolayer, which is similar to that of ODS.

Fluoroalkylsilane-based SAMs are widely used for hydrophobization of various surfaces [9,12,20,21], however, their formation mechanisms, which are expected to be analogous to those of alkylsilane SAMs, were not yet studied extensively. Moreover, the degree of self-assembly is normally ignored in the literature, when hydrophobic or superhydrophobic fluoroalkylsilane-SAM-grafted surfaces are concerned [9,12,14,16,20,22,23]. Furthermore, a perspective use of various SAM coatings as snow- and ice-repellent materials with low surface energy has been recently reported by several groups [10,24,25]. However, there is still a lack of systematic knowledge on how the microstructure and surface chemistry of SAMs influence the hydrophobic and, in particular, snow- and ice-repellent properties of the coatings. As SAMs of fluoroalkylsilanes are expected to demonstrate even lower surface energy compared to that of alkylsilanes, it is interesting to compare their hydrophobicity. The latter has been demonstrated to have a direct correlation with interfacial strength between SAM-grafted surfaces and ice [25].

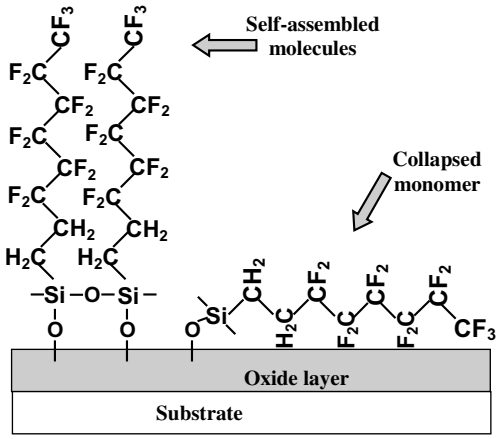

Fig. 1. 1H,1H,2H,2H-perfluorooctylsiloxane (FAS-13) monolayer on an oxide surface. Well-oriented, or self-assembled, (left) and collapsed (right) molecules are shown, exposing their topmost CF_3 and CF_2 (or CH_2) groups, respectively.

This paper presents a comparative analysis of wetting behavior of both smooth and rough surfaces covered with the most common fluoroalkylsiloxane (FAS-17 and FAS-13) and octadecylsiloxane (ODS) monolayers. Such SAMs can be formed from commercially available silanes, namely: 1H,1H,2H,2H-perfluorodecyltrimethoxysilane [7,9,14,16,20–22,26] or 1H,1H,2H,2H-perfluorodecyltrichlorosilane [12,23] (FAS-17); 1H, 1H,2H,2H-perfluorooctyltrichlorosilane [23] (FAS-13); and octadecyltrichlorosilane [5,15,17–19] (ODS). Another intention of the present work was to show the importance of the assembly order as an important factor governing hydrophobicity of SAM-coated surfaces. Both static (defined by the contact angle of water droplet) and dynamic (defined by the sliding angle) hydrophobicities are theoretically modeled as functions of self-assembly order/disorder degree and area fraction of air trapped by rough hydrophobic surfaces.

2. Model for calculations

The formation mechanism of fluoroalkylsilane SAMs was not investigated extensively and is likely to be similar to that of alkylsilane monolayers [5,15,17–19,27]. The analysis of literature shows that self-assembling of alkylsilanes occurs by the following steps. First, the molecules are hydrolyzed by water and form silanol-containing species. The OH groups of these silanols form hydrogen bonds to each other and to surface OH groups. Interactions between the alkyl chains direct chain ordering to form a well-organized and dense film. Finally, the organized monolayer is covalently grafted by the condensation reaction of the hydroxyl groups

to form Si–O–Si linkages within the monolayer and with the surface [5,13,15,17–19]. Depending on reaction conditions, the formation of complete monolayers with a dense, well-organized assembly with aligned alkyl chains, or the creation of a coating with disordered molecules that have not self-assembled to form condensed domains can be observed [15,17–19, 27]. In Fig. 1, disordered species (right) and a well-organized domain (left) are shown for a FAS-13 monolayer. The relative proportion of ordered and disordered phases depends on water and silane concentrations, solution age, chain length of silane molecules, temperature, exposure or reaction time, dispersion pH, substrate surface conditions, and steric effects [13,15,17–19,27]. Moreover, self-assembly is not the only reaction possible between alkylsilanes and surfaces; covalent attachment and vertical polymerization of silane monomers are also possible under certain conditions [27].

On the basis of the above, a model describing the wetting behavior of fluoroalkylsiloxane and alkylsiloxane monolayers with the following assumptions is proposed. (1) The distribution of heterogeneities is assumed to be uniform over the surface, irrespective of their chemical or geometrical character. (2) The effect of pores in coatings is negligible, and the surfaces are fully grafted by SAM molecules, which expose their CF_3 (or CH_3) and CF_2 (or CH_2) groups atop (see Fig. 1). (3) The wettability of a smooth fluoroalkylsilane- (or alkylsilane)-grafted surface is defined by relative contributions of CF_3 (or CH_3) and CF_2 (or CH_2) groups which interact with water. Well-assembled aggregates with vertically aligned fluoroalkyl (alkyl) chains are terminated by CF_3 (or CH_3) groups (Fig. 1, left), whereas CF_2 (or CH_2) groups start to be exposed when a continuous growth with formation of disordered submonolayer takes place (Fig. 1, right). (4) The parameters f_3 and f_2 are introduced as area fractions of CF_3 (CH_3) and CF_2 (CH_2)-terminated surface patches, respectively. Thus, coatings with high degrees of assembly are characterized by high values of f_3 and low values of f_2, provided that $f_3 + f_2 = 1$. (5) Rough surfaces and air inclusion in the surface structure are modeled by changing fractions of water and air-covered surface patches.

For the simplest cases of flat and chemically heterogeneous surfaces composed of N phases, the wettability can be evaluated from Eqs. (1) and (2), which are generalized cases of the Israelachvili-Gee [28] and Cassie [3] equations for N-phase surfaces with patch sizes of molecular and micrometer dimensions, respectively. Relation (1) is used whenever the size of chemically heterogeneous domains approaches molecular dimensions, while Eq. (2) describes surfaces composed of well-separated and distinct domains of micrometer size or larger. Both types of heterogeneity, with patch sizes of below and over 1 μm, have been demonstrated, e.g., for ODS monolayers on Si and mica substrates, and occur depending on process parameters [15,17–19].

$$(1+\cos\theta)^2 = \sum_{i=1}^{N} f_i(1+\cos\theta_i)^2 \tag{1}$$

$$\cos\theta = \sum_{i=1}^{N} f_i \cos\theta_i \tag{2}$$

Here, θ is the equilibrium contact angle of a chemically heterogeneous and ideally flat surface; θ_i contact angle for a pure homogeneous constituent phase with its area fraction f_i; $\sum_{i=1}^{N} f_i = 1$. Table 1 gives the contact angles for pure surfaces used in the present work. Recently, Eq. (1) has been used both experimentally and theoretically to describe the degree of order/disorder of hydrophobic coatings of water dispersible organosilane [13] or alkylsilane [30] coatings. It was shown by Almanza-Workman et al. that area fraction of experimentally obtained well-organized domains f_3 can reach 0.95 [13].

For completely wetted rough surfaces (Fig. 2a), Wenzel proposed a model to describe the contact angle θ_r considering the actual surface area [2].

Table 1
Water contact angles on certain pure surfaces

Surface	Contact angle, θ (°)	References
CF_3	120	[29]
CF_2	108	[6,29]
CH_3	111	[29]
CH_2	94	[13,29]

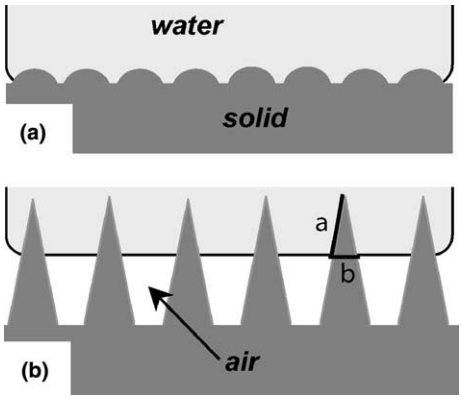

Fig. 2. (a) Schematic representation of wetting of hydrophobic solid surface at low roughness. (b) Air is entrapped beneath the water droplet on the surface after certain increase in roughness. Schematic illustration of the model surface composed of a series of uniform needles which is used for sliding angle calculations.

According to the model, Eqs. (1) and (2) are modified into Eq. (3):

$$\cos\theta_r = r\cos\theta \tag{3}$$

where r is a roughness factor, defined as the ratio of the actual area of a rough surface to its geometrically projected area [1,16,31].

When the roughness factor of a hydrophobic surface exceeds a certain value, the system switches its dominant wetting mode from Wenzel's (Fig. 2a) to Cassie's, in which the water does not penetrate into the troughs (Fig. 2b) [1,14,16,26,32]. Such surfaces are referred to as "composite" surfaces, since the intersection of the water droplet with the surface consists of a composite mixture of water–solid and water–air interface area. The wettability of such surfaces, provided that air is trapped as micro-pockets and $\cos 180^\circ = -1$, is expressed by Eq. (4):

$$\cos\theta_c = f^w\cos\theta - f^a = f^w\cos\theta + f^w - 1 \tag{4}$$

where θ_c is the contact angle of water on a "composite" surface with air trapped; f^w is the area fraction of the water-covered solid surface; and f^a is the area fraction of the air-covered solid surface.

For a water droplet on a rough hydrophobic and chemically heterogeneous surface consisting of CF_3 (CH_3) and CF_2 (CH_2)-terminated phases in Cassie's regime, Eq. (2) may be modified into Eq. (5) since the surface is partially covered with water:

$$\cos\theta^* = f_3\cos\theta_3^* + (1-f_3)\cos\theta_2^* \tag{5}$$

where "*" denotes a surface partially covered with air. As shown below (Fig. 3a), Eqs. (1) and (2) predict very close values of contact angles, therefore,

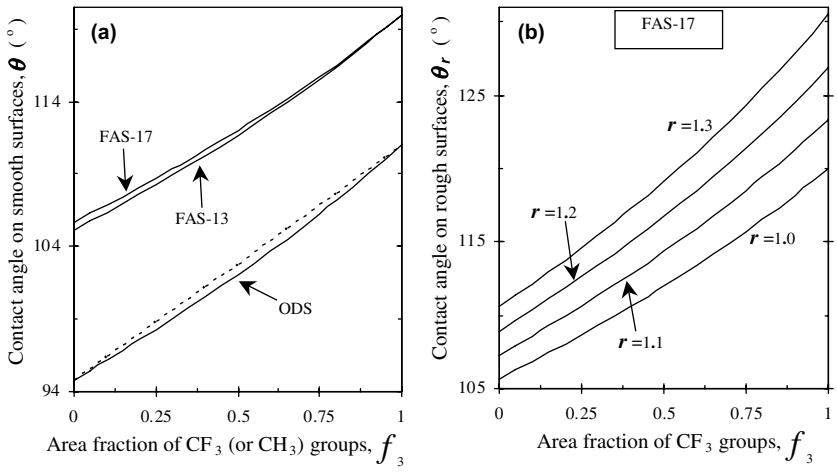

Fig. 3. Contact angle of water droplet on SAM-grafted surfaces as a function of assembly order/disorder degree. (a) Smooth surfaces with 1H,1H,2H,2H-perfluorodecylsiloxane (FAS-17), 1H,1H,2H,2H-perfluorooctylsiloxane (FAS-13), and octadecylsiloxane (ODS) monolayers. Dashed and solid lines indicate surfaces with micro-sized and nano-sized heterogeneous patches, respectively. (b) Effect of roughness for FAS-17 monolayers in Wenzel's wetting regime. Curves for nano-patches are presented.

for simplicity, Eq. (5) considers chemically heterogeneous surfaces with micro-sized patches. Further, the surfaces of both phases may be divided into two parts, one being covered with water and the other with air with the area fractions $f_3^w + f_3^a = 1$ and $f_2^w + f_2^a = 1$ for CF_3 (CH_3) and CF_2 (CH_2)-terminated domains, respectively. Here, superscripts "w" and "a" denote water and air, respectively. Thus, taking Eq. (4) into account, $\cos\theta_3^*$ and $\cos\theta_2^*$ may be expressed by Eqs. (6) and (7):

$$\cos\theta_3^* = f_3^w(1 + \cos\theta_3) - 1 \tag{6}$$

and

$$\cos\theta_2^* = f_2^w(1 + \cos\theta_2) - 1 \tag{7}$$

The combination of Eqs. (5)–(7) leads to Eq. (8), which describes the equilibrium contact angle of water on rough chemically heterogeneous surfaces of two phases formed by fluoroalkylsiloxane or alkylsiloxane monolayers with air trapped:

$$\cos\theta^* = f_3(f_3^w(1 + \cos\theta_3) - 1) + (1 - f_3)(f_2^w(1 + \cos\theta_2) - 1) \tag{8}$$

Because water droplets on a rough hydrophobic surface often reside in metastable states and thus exhibit metastable contact angles [14,22,32], the static contact angle alone is not sufficient to reflect the wettability of the surface. As was demonstrated experimentally, surfaces with high contact angles do not always show low sliding angles [32–34]. Therefore, when describing hydrophobicity, the sliding property of water droplets should also be evaluated and considered together with the contact angle [14,22,26,32,35]. Recently, sliding angles as low as ~1° (for a water droplet of 7 mg) [14] and 0.15° (droplet of 20 mg) [35] have been experimentally achieved on low-energy surfaces of FAS-17-coated boehmite [14] and of diamond-like carbon-polydimethylsiloxane hybrid coatings [35].

To qualitatively evaluate sliding angles of rough SAM-coated surfaces as a function of self-assembly f_3, we adopt Eq. (9), which was proposed by Miwa et al. [14] to describe sliding angles of water droplets on rough and uniform needle-like surfaces. Fig. 2b shows a schematic illustration of such a surface.

$$\sin\alpha = \frac{2Rk\sin\theta^*(\cos\theta^* + 1)}{g(R\cos\theta + 1)} \times \left(\frac{3\pi^2}{m^2\rho(2 - 3\cos\theta^* + \cos^3\theta^*)}\right)^{1/3} \tag{9}$$

In Eq. (9), α is the minimum angle at which a droplet begins to slide down the inclined surface; R is the ratio of the side area to the bottom area of a needle (defined by the ratio a/b in Fig. 2b); θ and θ^* are contact angles on smooth and rough "composite" surfaces, respectively; m and ρ are the mass and specific weight of a water droplet, respectively; g is the gravity acceleration; and k is a constant, which was related to the interaction energy between solid and liquid by Murase and Fujibayashi [33,34].

3. Results and discussion

3.1. Flat surface

The contact angle for completely disordered monolayers of fluoroalkylsiloxanes and alkylsiloxanes on smooth surfaces may be calculated from Eq. (1), which is for chemically heterogeneous surfaces with atomic- or molecular-sized domains. Contact angles for pure CF_3, CF_2, CH_3, and CH_2 surfaces are given in Table 1. For a 1H,1H,2H,2H-perfluorooctylsilane-grafted surface with completely collapsed monomers (Fig. 1, right) Eq. (1) is modified into Eq. (10):

$$\{1 + \cos\theta(\text{FAS-13})\}^2 = 0.1\{1 + \cos\theta(CF_3)\}^2 + 0.7\{1 + \cos\theta(CF_2)\}^2 + 0.2\{1 + \cos\theta(CH_2)\}^2 \tag{10}$$

From Eq. (10) θ (FAS-13) = 105.1°, which is somewhat lower that the water contact angle of 108° on pure polytetrafluoroethylene surface terminated with CF_2 goups [6,29]. Similarly, contact angles for completely disordered perfluorodecylsiloxane θ (FAS-17) and octadecylsiloxane θ (ODS) monolayers are obtained to be of 105.7° and 94.8°, respectievely. Note that the latter is somewhat higher than 94°, which was previously used for completely disordered alkylsilane SAMs [13,30].

Fig. 3a shows the influence of the degree of fluoroalkylsilane or alkilsilane self-assembly on the contact angle of a sessile water droplet, as calculated from Eq. (1). The three curves present the wetting behavior of flat surfaces coated with FAS-17, FAS-13, and ODS monolayers. As expected, perfluorodecylsilane-grafted surfaces demonstrate somewhat higher water contact angles than those of perfluorooctylsilane-grafted substrates at lower assembly degree (f_3). However, the difference, which is due to the number of exposed CF_2 and CH_2 groups, gradually decreases with an increase in assembly, since the surfaces start to expose mainly their topmost CF_3 groups at f_3 close to 1. The values of contact angles monotonically increase as the area fraction of well-organized (CF_3- or CH_3-terminated) patches increases, being larger for fluoroalkylsilane coatings. The maxima achieved on flat surfaces are equal to 120° and 111°, corresponding to the data for pure CF_3 and CH_3 surfaces, respectively (Table 1). This implies the importance of controlling the f_3 parameter when SAMs with improved water repellency are to be produced.

As reported previously [28,30] and as expected from Eqs. (1) and (2), for the same values of f_3 the predicted contact angles for surfaces of micro-sized patches are somewhat greater than for those of molecular-size patches; this is also shown in Fig. 3a by dashed and solid lines for ODS monolayers.

3.2. Rough surface and air inclusion

It is well known that water contact angles on smooth hydrophobic surfaces are not over 110–120° [5,6,29,36]. However, the situation is quite different when the surface is roughened. Fig. 3b shows that water contact angles of rough SAM-grafted surfaces in Wenzel's wetting regime, calculated using Eq. (3) for FAS-17 SAMs at $r = 1.1$, 1.2, and 1.3, increase constantly compared to those of smooth surfaces (curve marked with $r = 1.0$). Thus, rougher substrates enable to increase static water contact angles, and for well-organized fluorosiloxane monolayers the latter can exceed 120°. It is worth noting that surface roughness of hydrophobic SAM-coated substrates can be designed, e.g., by depositing underlayers of SiO_2 or Al_2O_3 with a desirable surface morphology [9], by means of substrate patterning [16,37], by sol–gel technique [26], or by plasma etching of the substrate before the SAM film is grafted [12].

The importance of air entrapped in the surface structure for achieving a high water contact angle has been emphasized by a number of research groups [1,14,16,26,32]. Figs. 4a–c show the relations between θ^* and f_3 and f_3^w, as calculated from Eq. (8) for FAS-17-grafted "composite" surfaces. Three different cases of water coverage of CF_2 (CH_2)-terminated domains with $f_2^w = 0.2$ (a), 0.5 (b), and 0.8 (c) are presented. It can be observed that higher values of θ^* are attained when f_3^w and f_2^w are lower, and the self-assembly order is improved (f_3 close to 1). When water-coverage fraction of CF_2 (CH_2)-terminated patches is increased (in Figs. 4a–c, $f_2^w = 0.2$, 0.5, and 0.8), the contact angle θ^* decreases. However its tendency, with respect to f_3 and f_3^w, remains the same as for lower values of f_2^w.

Fig. 4d compares contact angles on FAS-17, FAS-13, and ODS-grafted "composite" surfaces as a function of assembly order under water-coverage regime of $f_3^w = f_2^w = 0.5$. It is seen that contact angles on rough "composite" surfaces with water-coverage fraction of $f_3^w = f_2^w = 0.5$ are ~14–18.6° and ~21.8–28° higher for fluoroalkylsilane-grafted and ODS-grafted surfaces, respectively, if compared to those on smooth surfaces (Fig. 3a). The higher increase in contact angles on ODS-coated "composite" surfaces is partly a result of air inclusion into the water–solid interface. The surfaces in Fig. 4d are only partially (50%) in contact with water, the other 50% being in contact with air. It should also be mentioned that the condition of $f_3^w = f_2^w = 0.5$ for flouroalkylsilane and ODS-covered surfaces in Fig. 4d implies their water-coverage fractions to be equal, rather than equal geometrical topologies. We suppose that the ODS-grafted surfaces in Fig. 4d should have more "advantageous" topographies compared to those of FAS-17 (or FAS-13)-grafted ones to satisfy the same requirement of $f_3^w = f_2^w = 0.5$, as being higher-energy surfaces. For this reason, we believe that on substrates with same topographies a difference somewhat greater than that between the

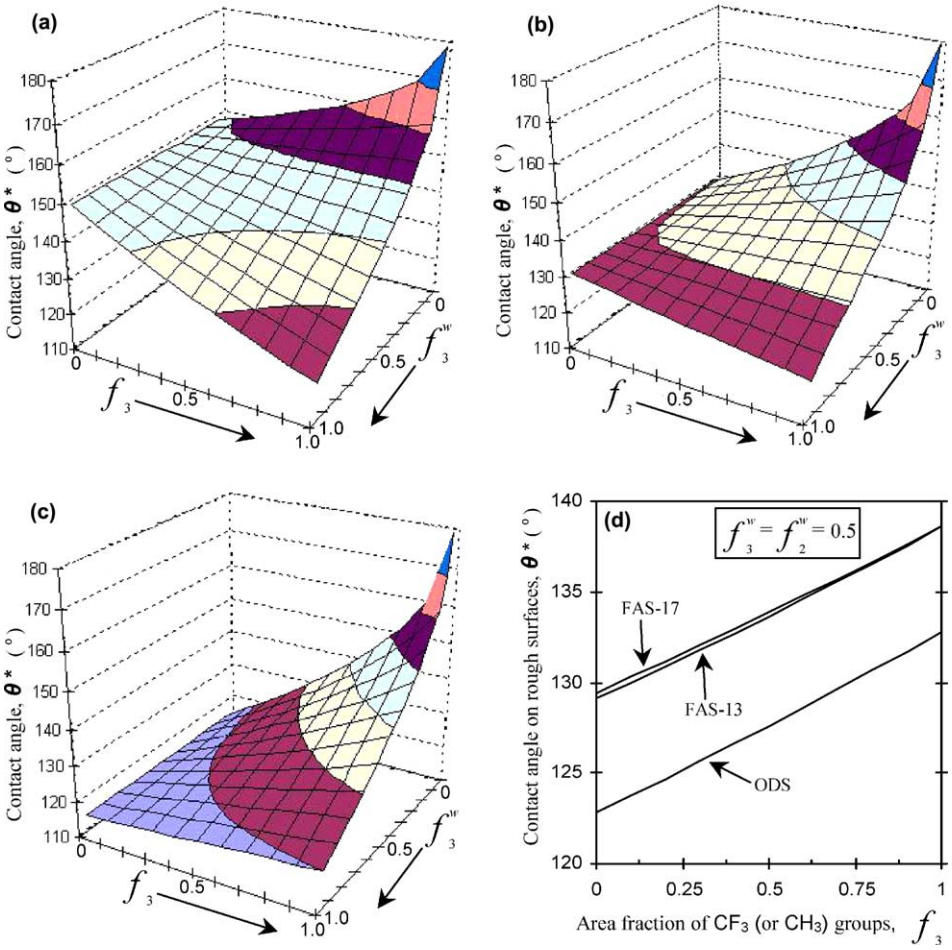

Fig. 4. (a)–(c) Contact angle of FAS-17-grafted rough "composite" surfaces as a function of SAM assembly order (f_3) and water coverage of CF_3-terminated patches (f_3^w). The water coverage of CF_2 (CH_2)-terminated patches (f_2^w) equals 0.2 (a); 0.5 (b); and 0.8 (c). (d) Comparison of wetting behavior of FAS-17, FAS-13, and ODS-grafted rough "composite" surfaces as a function of f_3 under water-coverage regime of $f_3^w = f_2^w = 0.5$.

curves in Fig. 4d should be expected, since a higher water-coverage regime for ODS-coated substrates should be realized (with deeper water penetration into surface troughs).

The same tendencies are observed in Figs. 5a–c, where the relation between θ^* and f_3^w and f_2^w is shown for three different assembly orders of FAS-17: $f_3 = 0.05$ (a), 0.5 (b), and 0.95 (c). Again, higher assembly order (f_3) and lower water coverage of CF_3-terminated (f_3^w) and CF_2 (CH_2)-terminated patches (f_2^w) result in higher values of equilibrium contact angle θ^*. As expected, the influence of water coverage of CF_2 (CH_2)-terminated domains is the most considerable at low self-assembly degree ($f_3 = 0.05$ in Fig. 5a), while it is very weak for well-assembled coatings ($f_3 = 0.95$ in Fig. 5c). It is also seen in Figs. 4a–c and 5a–c that contact angles of water much higher than 120° (maximum possible for a flat CF_3-terminated surface) can be achieved on rough surfaces under certain conditions.

Fig. 5d compares contact angles on FAS-17, FAS-13, and ODS-coated "composite" surfaces with low-organized monolayers ($f_3 = 0.05$) at

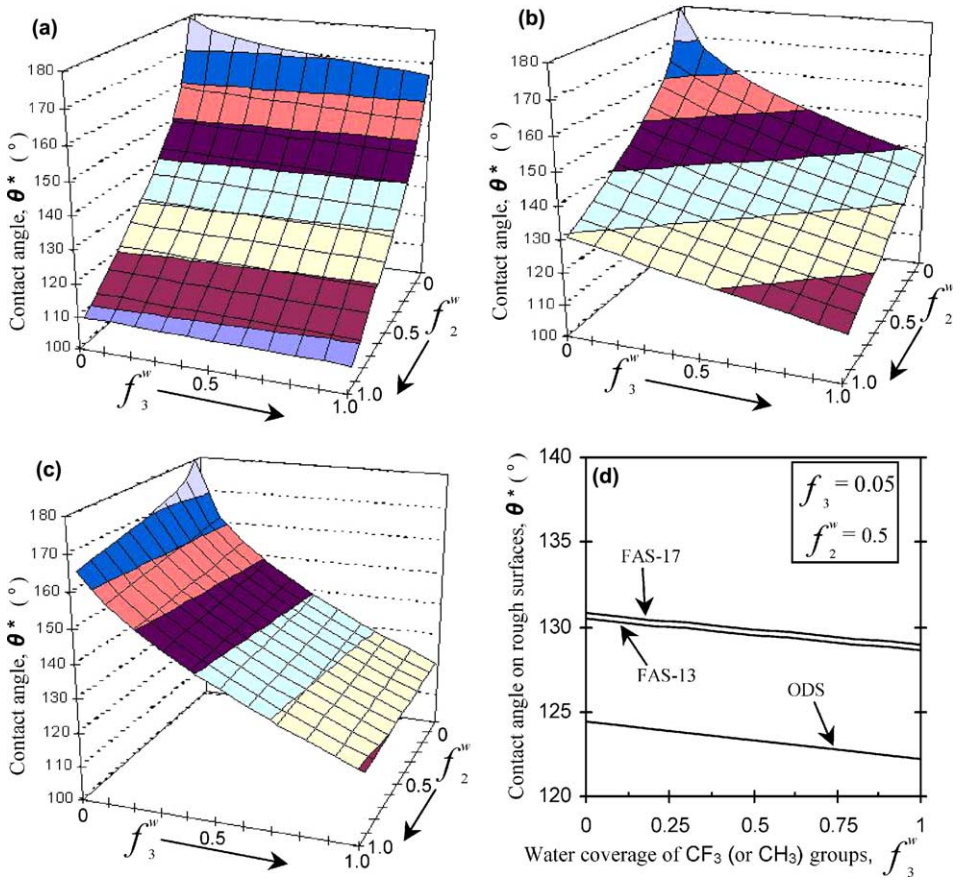

Fig. 5. (a)–(c) Contact angle of FAS-17-grafted rough "composite" surfaces as a function of water coverage of CF_3-terminated patches (f_3^w) and CF_2 (CH_2)-terminated patches (f_2^w). The self-assembly order (f_3) equals 0.05 (a); 0.5 (b); and 0.95 (c). (d) Comparison of wetting behavior of FAS-17, FAS-13, and ODS-grafted rough "composite" surfaces as a function of f_3^w at $f_2^w = 0.5$ and $f_3 = 0.05$.

$f_2^w = 0.5$ as a function of water-coverage fraction f_3^w. The difference in wetting of low-organized FAS-17 and FAS-13 monolayers is quite apparent. Note, however, as a CF_3 (CH_3)-terminated phase is more hydrophobic than a CF_2 (CH_2)-terminated one, any wetting regimes with $f_3^w > f_2^w$ are hardly expected [38]. Therefore, any materials described in Figs. 4 and 5 by parts of 3-dimensional surfaces or curves where $f_3^w > f_2^w$ are not to be realized in practice. Moreover, we believe that on SAM-grafted surfaces with nano-sized distribution of heterogeneities and micro-sized (or over) air inclusions the water-coverage conditions of $f_3^w \sim f_2^w$ should be expected.

3.3. Sliding angle on rough surfaces

Based on the assumption of uniform surface distribution of CF_3 (CH_3) and CF_2 (CH_2)-terminated patches, and assuming air inclusions at micrometer scale or over, it can be expected that on real SAM-grafted surfaces with air entrapped, the condition of $f_3^w \sim f_2^w$ will be realized. Therefore, sliding angles are evaluated only for FAS-17-grafted needle-like "composite" surfaces with $f_3^w = f_2^w$. Figs. 6a–c show sliding angles as functions of SAM assembly order (f_3) and water droplet mass (m). The three dependencies are given for FAS-17-coated "composite" surfaces on which the

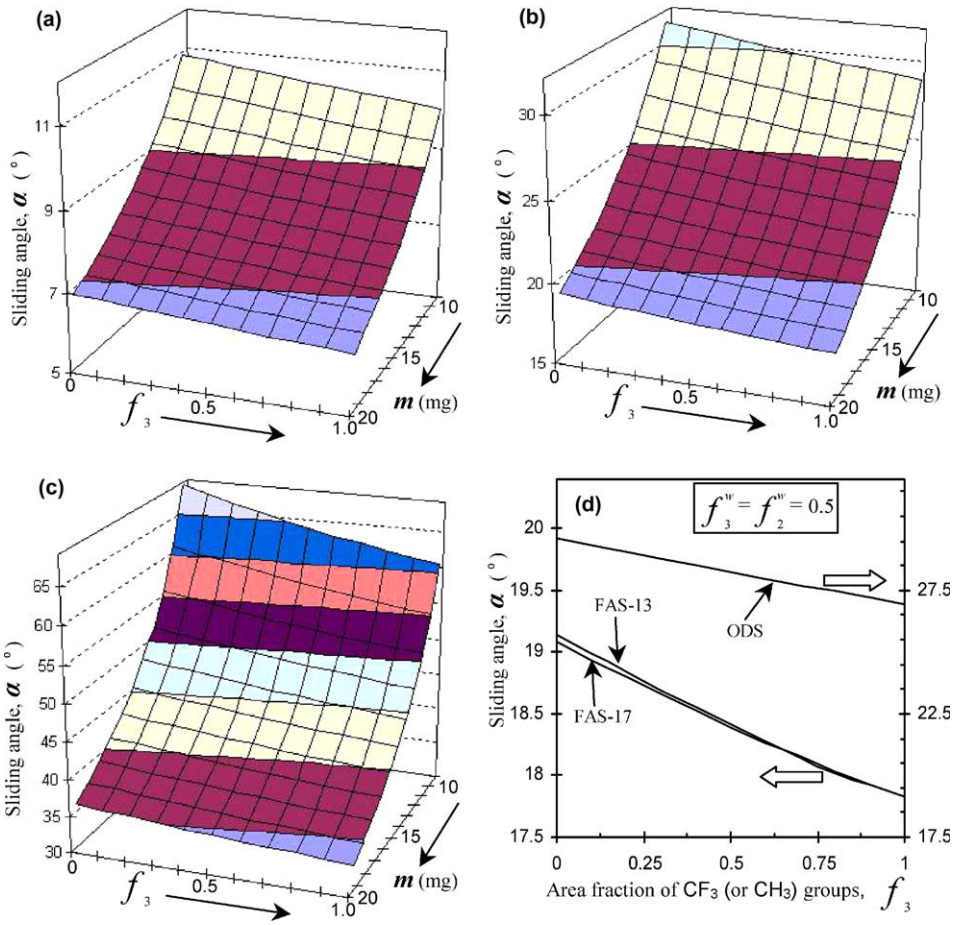

Fig. 6. (a)–(c) Sliding angle of FAS-17-grafted rough "composite" surfaces as a function of SAM assembly order (f_3) and mass of water droplet (m). The water coverage of CF_3 (CH_3) and CF_2 (CH_2)-terminated patches ($f_3^w = f_2^w$) equals 0.25 (a); 0.5 (b); and 0.75 (c); the R parameter of the needle-like structures is 1.15. (d) Comparison of sliding angles for a water droplet of 20 mg on FAS-17, FAS-13, and ODS-grafted rough "composite" surfaces of uniform needles as a function of f_3 under water-coverage regime of $f_3^w = f_2^w = 0.5$.

water–solid interface conditions of $f_3^w = f_2^w$ equal to 0.25 (a), 0.5 (b), and 0.75 (c) are realized. The results were obtained by using Eq. (9) in combination with Eqs. (1) and (8) for surfaces with $R = 1.15$ and for water droplets from 10 to 20 mg, in accordance with the surface model of Miwa et al. [14], schematically shown in Fig. 2b. For simplicity, the constant k was chosen to be equal to 12.49 mJ/m^2 and independent of the FAS-17 assembly degree. This value was reported by Miwa et al. as the experimental constant for flat FAS-17-coated glass [14]. We believe this value represents the interaction between water and well-assembled FAS-17 siloxane monolayers, although the authors of Ref. [14] have not reported any data on the assembly degree of their coatings.

Comparing Figs. 6a–c, one can conclude that lower water sliding angles may be attained on hydrophobic surfaces with low fractions of water coverage for both CF_3 and CF_2 (CH_2)-terminated domains, f_3^w and f_2^w. Because of high air ratio at the water–solid interface, sliding resistance of such surfaces is reduced, giving rise to lower sliding

angles. Increased water droplet mass improves sliding ability of the surfaces in Figs. 6a–c irrespective of their water coverage, i.e., heavier droplets slide down easier. It is also seen that increasing f_3 leads to reduced water sliding angles, thus improving surface dynamic hydrophobicity.

As any data on the interaction constant k for the water-alkylsilane SAM system are missing, it is impossible to present simulation results for sliding angles on ODS-grafted rough surfaces similar to those in Figs. 6a–c. Fig. 6d, however, qualitatively compares sliding angles of water droplets with $m = 20$ mg on "composite" FAS-17, FAS-13, and ODS coatings as functions of SAM assembly degree at $f_3^w = f_2^w = 0.5$. Here, to evaluate sliding behavior of ODS monolayers, $k = 17.8\,mJ/m^2$ is used, which is the experimental constant for the water-polypropylene system [39] and is assumed to be a reliable value for water-alkylsiloxane monolayer interactions (also defined by CH_2 and CH_3 surface groups exposed).

Strictly speaking, as being related to the interaction energy between a solid surface and water [14,33,34,39], the constant k should be f_3 dependent. Representing the surface energy of a solid, k is expected to be slightly larger for coatings with low values of f_3 and lower for those with high f_3. Such a f_3 dependent value of k is expected to result in somewhat greater sliding angles at low f_3 and lower ones at f_3 close to 1 (see Eq. (9)).

Note that, similarly to Fig. 4, the 3-D surfaces presented in Fig. 6 describe surface structures with same water-coverage parameters rather than with same geometrical topographies. For example, Figs. 6a–c describe sliding behavior of FAS-17-grafted uniform needle-like surfaces with area fractions of water–solid interface ($f_3^w = f_2^w$) equal to 0.25, 0.5, and 0.75, respectively. Consequently, when topologically equal needle-like substrates are coated with SAMs with different self-assembly order f_3, water will tend to penetrate less between the needle-like posts with higher f_3. Thus, to keep the water-coverage parameters constant at higher values of f_3, the topography of the substrate should be "adjusted"; in the simplest case of constant needle geometry and uniform needle-like structure, the distance between the needles should be increased, thus allowing water to penetrate deeper along the needles and satisfy the requirement of constant water–solid interface fraction ($f_3^w = f_2^w = \text{const}$). And vice versa, keeping the substrate topography constant, at increased assembly order of SAM coatings, one should expect a constant decrease in water coverage of the surface ($f_3^w = f_2^w$ decreases). As a result, sliding behavior of water on such surfaces will be more f_3 dependent than can be observed in Figs. 6a–d for constant $f_3^w = f_2^w$. Thus, Fig. 6 is only a very qualitative approximation, allowing, however, to reveal the character and tendencies of sliding behavior of "composite" surfaces with fluoroalkylsiloxane and alkylsiloxane monolayers and to compare them.

It should also be mentioned that the approach used in this study does not account for the geometry/topography of the surfaces under consideration. To date, there has been only limited research on how surface shapes and dimensions (roughness topography) influence static and/or dynamic hydrophobicity of rough surfaces [14,16,32]. The topological nature of the surface roughness is of prime importance in determining hydrophobicity; a proper interval and height difference in the microstructure are required to provide both high contact angles and low sliding angles on rough hydrophobic surfaces [14,32,40]. According to the recent approach of Chen et al. [32], to decrease water sliding angle, a properly designed surface is expected to not allow a continuous contact of a liquid with the surface and to demonstrate little or no difference in energy between different metastable states. As a result, the liquid droplet would not remain pinned in a metastable state and would move spontaneously on such a surface. Thus, additional work, combining both experimental and theoretical approaches, is needed to further understand the effect of roughness topography on wetting of hydrophobic SAM-coated surfaces.

3.4. Snow and ice repellency of SAM coatings

Finding low-energy surfaces or coatings and introducing air between the ice and substrate stand among the major strategies to reduce ice/surface adhesion that have previously been proposed in

the literature [24,25,30,41]. As low-surface-energy coatings, certain alkylsilane SAMs have recently attracted attention of investigators in this field. According to the recent results of Somlo and Gupta [24], ice adhesion decreases when a SAM is formed from dimethyl-*n*-octadecilchlorosilane on an Al alloy substrate [24]. Furthermore, Petrenko and Peng have found good correlation between the contact angle of water and ice-adhesion strength on surfaces covered with mixtures of SAMs of 11-hydroxylundecane-1-thiol and 1-dodecanethiol with various degrees of hydrophobicity/hydrophilicity [25].

Taking the above into consideration, the following conclusions can be drawn. (1) The formation of monolayers with high assembly degree [13,15,17–19] seems to be an important factor governing surface hydrophobicity and, probably, snow and ice repellency. As shown above, this improves both static and dynamic water repellency. While this parameter is often ignored in the literature [12,14, 16,20,24], one of the main objectives of this work was to demonstrate the importance of controlling the assembly degree of SAM coatings, when fluoroalkylsiloxane and alkylsiloxane-grafted surfaces with high hydrophobicity are to be produced. (2) Fluorinated alkylsiloxane monolayers are expected to be more advantageous and efficient compared to alkylsiloxanes, giving rise to surfaces with higher static and dynamic hydrophobicity. (3) The use of rough or patterned surfaces [9,12,16,26,37] as substrates for hydrophobic SAMs, so as to entrap air into the final surface structure, appears to be perspective as well. As was shown in the previous sections, higher contact angles and reduced sliding angles can be attained on such surfaces with an increase in air inclusion. This conclusion is in good agreement with the experimental results of Saito et al. [41], who have reported a linear correlation between the contact angle of water and ice adhesion strength for rough "composite" water-repellent coatings of polytetrafluoroethylene particles dispersed in polyvinylidene fluoride resin binder. Thus, properly designed/patterned rough fluoroalkylsiloxane or alkylssiloxane-coated surfaces are also expected to be good candidates for ice-repellent applications, too.

4. Summary

A model is presented to describe the wetting behavior of hydrophobic organic coatings of SAM molecules as a function of their self-assembly and amount of air trapped between water and solid. The model is applied to compare wetting of surfaces fully coated with fluorinated alkylsiloxane and alkylsiloxane monolayers. The contact angle of a sessile water droplet, as a measure of static hydrophobicity, is demonstrated to be $\sim 10^\circ$ higher on flat fluoroalkylsilane-grafted surfaces and to gradually increase with the assembly order. The difference, however, decreases when rough substrates with air inclusion are used. The results of modeling predict very close values of contact angles on surfaces coated with perfluorodecylsiloxane and perfluorooctylsiloxane SAMs, however, demonstrating little difference at low self-assembly degree, when organic molecules are spread on the surface and their CF_2 and CH_2 groups start exposing and interacting with water. At the same time, octadecylsiloxane coatings always show lower values of contact angle, which is due to the higher energy of CH_3 and CH_2-terminated surfaces compared with that of CF_3 and CF_2-terminated ones. It is demonstrated that both static (defined by the contact angle) and dynamic water repellency (defined by the sliding angle) of SAM-coated surfaces are strongly affected by the degree of self-assembly of fluoroalkylsilane or alkylsilane molecules and by water coverage of a rough surface, which can trap air. Increasing the assembly order of SAM molecules, in combination with properly designed roughness, leads to considerably improved hydrophobicity of the surface. Further detailed analysis, involving both experimental and theoretical approaches, is required for further understanding and improvement of hydrophobicity and snow/ice repellency of fluoroalkylsiloxane and alkylsiloxane monolayers on various surfaces.

Acknowledgments

This work was carried out under the sponsorship of the Natural Sciences and Engineering Research Council (NSERC) and Hydro-Quebec.

The authors wish to thank the sponsors of the project.

References

[1] A. Nakajima, K. Hashimoto, T. Watanabe, Monatsh. Chem. 132 (2001) 31.
[2] R.N. Wenzel, Ind. Eng. Chem. 28 (1936) 988.
[3] A.B.D. Cassie, Discuss. Farad. Soc. 3 (1948) 11.
[4] D.R. Bassett, J. Coat. Technol. 73 (2001) 42.
[5] K.-H. Cha, D.-E. Kim, Wear 251 (2001) 1169.
[6] J.-D. Kim, H. Sugimura, O. Takai, Vacuum 66 (2002) 379.
[7] H.-J. Jeong, D.-K. Kim, S.-B. Lee, S.-H. Kwon, K. Kadono, J. Colloid Interf. Sci. 235 (2001) 130.
[8] A. Hozumi, O. Takai, Thin Solid Films 303 (1997) 222.
[9] Y. Wu, H. Sugimura, Y. Inoue, O. Takai, Thin Solid Films 435 (2003) 161.
[10] M. Futamata, X. Gai, H. Itoh, Vacuum 73 (2004) 519.
[11] R.K. Smith, P.A. Lewis, P.S. Weiss, Prog. Surf. Sci. 75 (2004) 1.
[12] K. Ogawa, M. Soga, Y. Takada, I. Nakayama, Jpn. J. Appl. Phys. 32 (1993) L614.
[13] A.M. Almanza-Workman, S. Raghavan, S. Petrovic, B. Gogoi, P. Deymier, D.J. Monk, R. Roop, Thin Solid Films 423 (2003) 77.
[14] M. Miwa, A. Nakajima, A. Fujishima, K. Hashimoto, T. Watanabe, Langmuir 16 (2000) 5754.
[15] C. Carraro, O.W. Yauw, M.M. Sung, R. Maboudian, J. Phys. Chem. B 102 (1998) 4441.
[16] Z. Yoshimitsu, A. Nakajima, T. Watanabe, K. Hashimoto, Langmuir 18 (2002) 5818.
[17] D.K. Schwartz, S. Steinberg, J. Israelachvili, J.A.N. Zasadzinski, Phys. Rev. Lett. 69 (1992) 3354.
[18] D.W. Britt, V. Hlady, J. Colloid Interf. Sci. 178 (1996) 775.
[19] T. Vallant, H. Brunner, U. Mayer, H. Hoffmann, T. Leitner, R. Resch, G. Friedbacher, J. Phys. Chem. B 102 (1998) 7190.
[20] A. Nakajima, A. Fujishima, K. Hashimoto, T. Watanabe, Adv. Mater. 11 (1999) 1365.
[21] A. Nakajima, K. Hashimoto, T. Watanabe, K. Takai, G. Yamauchi, A. Fujishima, Langmuir 16 (2000) 7044.
[22] S. Suzuki, A. Nakajima, Y. Kameshima, K. Okada, Surf. Sci. 557 (2004) L163.
[23] S. Shibuichi, T. Yamamoto, T. Onda, K. Tsujii, J. Colloid Interf. Sci. 208 (1998) 287.
[24] B. Somlo, V. Gupta, Mech. Mater. 33 (2001) 471.
[25] V.F. Petrenko, S. Peng, Can. J. Phys. 81 (2003) 387.
[26] A. Nakajima, K. Abe, K. Hashimoto, T. Watanabe, Thin Solid Films 376 (2000) 140.
[27] A.Y. Fadeev, T.J. McCarthy, Langmuir 16 (2000) 7268.
[28] J.N. Israelachvili, M.L. Gee, Langmuir 5 (1989) 288.
[29] E.L. Decker, S. Garoff, Langmuir 13 (1997) 6321.
[30] S.A. Kulinich, M. Farzaneh, Appl. Surf. Sci. 230 (2004) 232.
[31] D. Quéré, Physica A 313 (2002) 32.
[32] W. Chen, A.Y. Fadeev, M.C. Hsieh, D. Öner, J. Youngblood, T.J. McCarthy, Langmuir 15 (1999) 3395.
[33] H. Murase, K. Nanishi, H. Kogure, T. Fujibayashi, K. Tamura, N. Haruta, J. Appl. Polym. Sci. 54 (1994) 2051.
[34] H. Murase, T. Fujibayashi, Prog. Org. Coat. 31 (1997) 97.
[35] M. Kiuru, E. Alakoski, Mater. Lett. 58 (2004) 2213.
[36] T. Nishino, M. Meguro, K. Nakamae, M. Matsushita, Y. Ueda, Langmuir 15 (1999) 4321.
[37] Y. Xia, D. Qin, Y. Yin, Curr. Opin. Colloid Interf. Sci. 6 (2001) 54.
[38] P. Lenz, Adv. Mater. 11 (1999) 1531.
[39] E. Wolfram, R. Faust, Liquid drops on a tilted plate, contact angle hysteresis and the Young contact angle, in: J.F. Padday (Ed.), Wetting, Spreading and Adhesion, Academic Press, London, 1978, p. 213.
[40] H. Nakae, R. Inui, Y. Hirata, H. Saito, Acta Mater. 46 (1998) 2313.
[41] H. Saito, K. Takai, G. Yamauchi, Surf. Coat. Int. 80 (1997) 168.